Original Research

Tracking Planar Orientations of Active MRI Needles

Shashank Sathyanarayana, MS,[1] Pelin Aksit, MS,[2] Aravind Arepally, MD,[3] Parag V. Karmarkar, MS,[3] Meiyappan Solaiyappan, MS,[3] and Ergin Atalar, PhD[3,4]*

Purpose: To determine and track the planar orientation of active interventional devices without using localizing RF microcoils.

Materials and Methods: An image-based tracking method that determines a device's orientation using projection images was developed. An automated and a manual detection scheme were implemented. The method was demonstrated in an in vivo mesocaval puncture procedure in swine, which required accurate orientation of an active transvascular needle catheter.

Results: The plane of the catheter was determined using two projection images. The scan plane was adjusted automatically to follow the catheter plane, and its orientation with respect to a previously acquired target plane was displayed. The algorithm facilitated navigation for a fast and accurate puncture.

Conclusion: Using image-based techniques, with no mechanical design changes, the orientation of an active intravascular probe could be tracked.

Key Words: interventional MRI; catheter tracking; projection images; active devices; loopless antenna
J. Magn. Reson. Imaging 2007;26:386–391.

TRACKING AND VISUALIZATION OF INTERVENTIONAL DEVICES is essential for procedures guided by real-time MRI, such as the mesocaval puncture procedure (1). In this procedure, a transvascular puncture is made from the inferior vena cava (IVC) to the superior mesenteric vein (SMV) using a needle catheter under real-time MR guidance. The catheter is designed to serve the dual purpose of a mechanical puncture needle as well as an MR receiver coil. Visualizing extended lengths of the needle is essential as it is advanced into the body, and tracking its orientation at the puncture point is critical for making a successful puncture.

Both passive and active techniques have been devised to visualize extended lengths of interventional devices (2). Passive techniques that use signal voids suffer from a low signal-to-noise ratio (SNR), and techniques such as gadolinium-filled catheters or MR-visible coated catheters (3,4) may render the catheter lumen unusable for additional device delivery and may require additional manufacturing processes. Active catheters incorporate MRI receiver coils, and extended lengths of devices can be visualized using designs such as the elongated-loop coil (5) and loopless antenna (6). These do not increase the catheter's size and are more conspicuous than passive catheters as they inherently localize signal, thereby improving contrast of the vasculature with respect to the surrounding anatomy. The loopless-antenna design can be further modified to incorporate the mechanical properties required—an elongated rigid shaft and a sharp tip for puncture procedures.

In addition to visualizing extended lengths, there is also a need to track the probe's orientation. Interventional device tracking has been performed previously (7,8), where one or more RF microcoils are incorporated in the catheter design and a special pulse sequence is used to localize the coils in 3D space. When multiple coils are incorporated, one can determine the orientation of the device by localizing the three coils, followed by automatic scan plane adjustment (9,10). However, including microcoils on the catheter may make it rigid and unsuitable for certain intravascular procedures. For example, in the mesocaval puncture procedure, a coil cannot be incorporated at the distal needle tip since the catheter must have a sharp end to make a puncture. In addition, only the particular locations that have the embedded coils can be used for tracking. However, the tip, along with its distal section, forms a vital portion of the catheter that must be tracked and visualized, necessitating an approach without the use of localizing coils. Furthermore, small-diameter catheters (0.014-

[1]Department of Electrical and Computer Engineering, Johns Hopkins University, Baltimore, Maryland, USA.
[2]Global Applied Science Laboratory, GE Healthcare, Waukesha, Wisconsin, USA.
[3]Russell H. Morgan Department of Radiology and Radiological Science, Johns Hopkins University School of Medicine, Baltimore, Maryland, USA.
[4]Department of Electrical and Electronics Engineering, Bilkent University, Ankara, Turkey.
Contract grant sponsor: National Institutes of Health; Contract grant numbers: R01-HL61672; K08 EB004348-01.
*Address reprint requests to: E.A., Department of Electrical and Electronics Engineering, Bilkent University, TR-06800, Bilkent, Ankara, Turkey. E-mail: ergin@ee.bilkent.edu.tr
Received February 27, 2006; Accepted January 25, 2007.
DOI 10.1002/jmri.20960
Published online in Wiley InterScience (www.interscience.wiley.com).

inch) can be constructed using designs such as the loopless antenna (11), which could be difficult using the microcoils approach.

Image-based catheter-tracking algorithms have been explored using device-only, thick-slab projections (12). This has been combined with volumetric MRI to visualize the device with regard to the surrounding anatomy (13) and to determine the direction toward which the probe is moving. In many applications, however, in addition to knowing this direction, we need to know the orientation of the entire device or at least of enough portions to monitor it. Projection imaging combined with manual scan plane adjustment (14) may be used, but does not explicitly ensure that the scan plane contains the device's portion of interest. In addition, this method requires a continuous update of the current scan plane in a feedback loop, with an associated increase in time and complexity.

Thus, there is a need to directly and accurately obtain the orientation and location of the interventional device with regard to its surroundings without using localizing RF coils. We describe a method that directly determines the plane of a catheter using two orthogonal projection images of the device. Once the plane of the catheter is determined, we automatically drive the scanner to the new plane and calculate its orientation with respect to an initially prescribed target plane. We demonstrate the method in an MR-guided mesocaval puncture performed in vivo using an active intravascular needle system. Previously, navigation in this procedure required acquisition of multislice images of the catheter and determination of the catheter position in complex anatomy. Our approach provides an efficient alternative to this cumbersome and complicated navigation. The approach can also be extended to other procedures that require the catheter position to be determined quickly and accurately.

MATERIALS AND METHODS

Catheter designs vary considerably depending on their use in interventional procedures. They may be thin and flexible for coronary interventions, or soft and pliable (e.g., neurocatheters) or rigid and hard for puncture procedures. The geometry of the particular device can be used to aid in its localization and tracking.

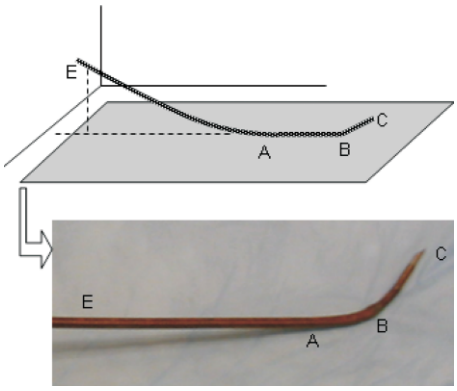

Figure 1. Top: Geometry of the catheter needle used in the mesocaval puncture procedure. The A-B-C portion lies in one plane, while the rest of the body (E-A) may not. Bottom: Depiction of the actual catheter used in the procedure.

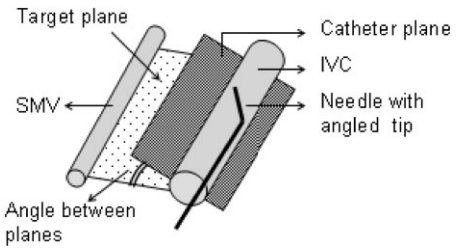

Figure 2. Simple depiction of the mesocaval puncture procedure and the need for plane tracking. The catheter must be rotated to the target plane by a specific angle for the puncture.

The needle catheter utilized in the mesocaval puncture procedure has a long rigid structure with an angled tip. The distal portion, along with the angled tip (A-B-C in Fig. 1), lies in one plane within the imaging slice thickness. This plane is referred to hereafter as the "catheter plane." While portions of the catheter may not lie in this plane (portion E-A in Fig. 1.), the planar orientation of the "relevant portion" (A-B-C) is vital because a puncture is enabled when the angled tip is oriented correctly from the IVC toward the SMV (Fig. 2). If the catheter plane is correctly calculated and displayed, it can aid in achieving a successful puncture. In addition, if the two veins are coplanar in a "target plane" and intersect the catheter plane along the catheter's axis, valuable information can be obtained by determining the angle between the catheter plane and the target plane. A simple rotation of the catheter about its axis would orient the tip correctly for the puncture. Although in the mesocaval puncture procedure the IVC and the SMV are almost coplanar at the puncture point, it is likely that a target plane, as described here, does not always exist. The vessels may not be coplanar, or the notion of a target plane may not exist. However, display of the catheter plane can provide, by itself, valuable navigational information for interventional procedures.

Algorithm

The determination of the plane containing the catheter is demonstrated in Fig. 3. The catheter ABC lies in a plane oriented at an arbitrary angle with respect to the coordinate axes, which must be determined. Further, if a target plane has been defined, its orientation with the catheter plane must also be calculated.

The coordinates of the catheter in 3D space are determined using the correspondence between its two-dimensional (2D) projection images (Fig. 3, top). Reconstruction of arbitrary three-dimensional (3D) shapes from 2D projections has been studied extensively (15). A simple case exists when the device has a linear structure, as in the puncture needle used in our procedure. Two projections obtained from different angles are sufficient to rebuild the device in 3D space. This can be further simplified if the projections are orthogonal to each other, since a direct correspondence exists be-

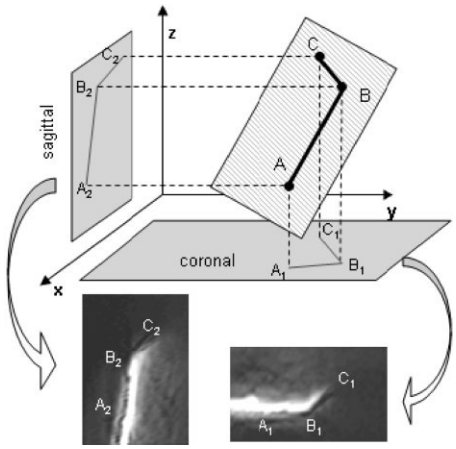

Figure 3. Top: Geometry for catheter plane reconstruction from orthogonal projections. Bottom: Sample projection images.

tween the projections (e.g., they share a common x-axis). As long as the catheter shape does not involve loops (i.e., it has a linear structure), each point in 3D space has a unique projection on the two orthogonal planes. When loops are involved, multiple points can have the same projection, and algorithms are required to resolve this ambiguity (16,17). Since we are interested only in the catheter's plane and not its entire shape, three noncollinear points located on the projection images are sufficient to define the catheter plane. The MR-active needle design ensures high contrast between its projections and the surrounding anatomy (Fig. 3, bottom). The geometry of the angled tip makes it convenient to find three noncollinear points (e.g., A_1, B_1, and C_1) on the projections, and a plane containing these three points can be calculated. In addition, the angled tip ensures that in cases where one projection shows a straight line, the other projection will have three noncollinear points. The calculated plane is automatically passed to the scanner in a standard 4×4 transformation matrix (18), and the orientation of the catheter plane is determined with respect to the initially prescribed target plane. In our procedure, the two planes share an axis along the length of the catheter (Fig. 2). Thus, in calculating the transformation matrix, the frequency-encoding direction for the catheter plane is set to that of the target plane. A simple rotation of the catheter by the calculated angle makes it coincident with the target plane. As a result, the physician has positional information, since the scanner now shows the catheter plane, as well as the device's orientation, since the angle between the catheter plane and target plane is displayed.

Automatic Detection

Since manual detection of points on the projections can be inefficient in the algorithm described above, automated detection strategies were explored. The catheter used in our experiment contains a receive-only antenna, and signal cancellations occur due to the interaction of its circular reception field with the homogeneous field of the transmit body coil (12). In projection images (e.g., a coronal projection), complete phase cancellation occurs perpendicularly above the catheter, while the cancellation is incomplete as we move away from the catheter along the field of view (FOV). Thus, the catheter has a dark center line with bright bands adjacent to it (Fig. 3, bottom). This rapid change in contrast was used to detect the catheter automatically. We used a "window" 20 pixels wide to scan each row of the projection, sliding 5 pixels at a time, noting the difference between the maximum and minimum values within the window as the "contrast." The area that shows maximal contrast change is the catheter. With a 28-cm FOV, the window and sliding length corresponded to 2.2 cm and 0.5 cm, respectively. These parameters were chosen empirically after the algorithm was tested on seven pairs of in vivo sagittal-coronal projections. The animal was advanced head-first into the scanner and the catheter was inserted using a femoral-vein approach. Scanning a projection from the top downward thus ensured that the first point detected was the tip of the catheter. The second point was detected using known physical tip dimensions, and the point on the shaft was offset such that the three detected points were equidistant.

Materials

All experiments were performed on a GE Signa 1.5T scanner (GE Medical Systems, Waukesha, WI, USA). A modified real-time user interface and pulse sequence provided orthogonal projection images and direct control of the scan plane. An active loopless-antenna catheter in receive-only mode was used as the puncture needle (Fig. 1). The antenna needle, which was manufactured in our laboratory, consists of concentrically configured nitinol hypotubings arranged to form a loopless antenna (6). The antenna needle has two, thin-walled, nitinol tubes with a central lumen that can accommodate a 0.038-inch guidewire over which the antenna can be safely advanced. The needle system has a caliber of 9F, with a sharpened bevel at the end. To facilitate punctures, the shaft is preshaped at the distal tip to provide a 55°, 3-cm bend (B-C in Fig. 1). The proximal end (not shown) is connected to the RF tune and match circuitry. Except for the distal tip of the tube, the entire assembly is insulated with nylon to isolate the needle components from direct electrical contact with biologic fluids. A four-channel GE cardiac array, combined with the catheter and an in-house-developed interface box, was used to obtain anatomical images. A modified real-time steady-state free precession (SSFP) sequence with real-time control of lipid suppression and inversion recovery (IR) was developed for improved visualization of the catheter and the anatomy. Typical imaging parameters were TR/TE/FA = 4 msec/1 msec/45°, frames per second (fps) = 6–8, slice thickness = 5 mm, matrix = 224×128, FOV = 30 cm, and BW = 62.5 kHz. Some of these parameters were dynamically modified during the procedure. For example, lipid suppression or IR preparations were used to suppress background tissues and accentuate the device, and the FOV varied between 16 cm and 32 cm

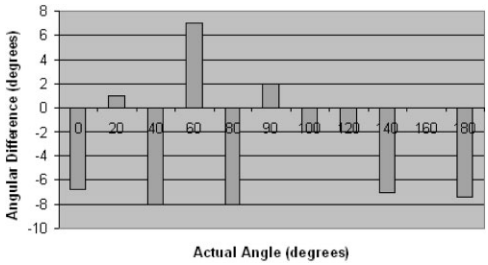

Figure 4. Angular difference between calculated and actual angles in a phantom positioned on the scanner table at the center of the bore.

during the in vivo procedure depending on the required resolution. The use of an IR preparation reduced the frame rate to approximately 1 fps when assessment of the tissue around the needle was desired. The algorithm to calculate the device plane was implemented as a Graphical User Interface (GUI) in MATLAB (Mathworks Inc., Natick, MA, USA) on a Linux PC connected by 100baseT Ethernet to the scanner console, with file transfer automated using PERL's FTP package (Perl Foundation, Ann Arbor, MI, USA), which provided adequate speed for our procedure. The system configuration is further explained in the Results section.

Phantom Experiments

Experiments were performed on an active loopless-antenna catheter immersed in a trough of water to test the accuracy of the proposed method. Automatic detection parameters were not optimized for the phantom experiments, and manual detection was used. The target plane was defined as the coronal plane. The catheter was rotated such that the plane passing through the distal tip (the "catheter plane") created known angles with the target plane from 0° to 180°, in steps of 20°. The difference between the actual angle, measured by a protractor, and the calculated angle provided by the algorithm was noted (Fig. 4). The average difference was less than 5°. Mechanical torsion between the distal tip and proximal end at which the protractor was placed can lead to the repeated underestimation of calculated angles as tabulated. For the 30-mm distal bend, the 8° maximum error corresponds to a tip mislocation of 4 mm (30sin8°). Since this is within the imaging slice thickness of 5 mm, the results were considered acceptable.

RESULTS

With approval from the institutional animal care and use committee, two in vivo mesocaval puncture procedures in swine were guided using our algorithm. The active catheter puncture needle was introduced from the common femoral vein through a standard 12F vascular sheath and advanced over a 0.035-inch nitinol guidewire (EV3, Plymouth, MA, USA). During the procedure, the interventionalist advanced the needle by using an imaging console adjacent to the MR unit to monitor the needle and its orientation. The target plane, containing both the IVC and SMV, was initially pre-

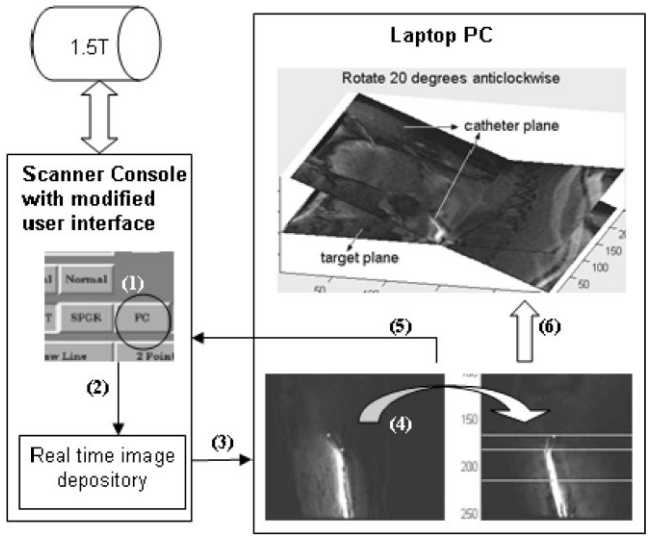

Figure 5. System architecture showing the steps in the localization procedure: 1) update requested, 2) projections acquired and stored, 3) images transferred to PC and displayed, 4) device located on projections and 3D position found, 5) catheter plane fed back to scanner, and 6) orientation of catheter plane with respect to target plane displayed.

scribed and stored using a set of axial scout scans. Modifications to the real-time interface provided coronal and sagittal projections of the catheter channel. Since the catheter was predominantly along the long axis of the scanner bore, axial projections were not preferred as they can contain difficult-to-resolve overlaps of the tip and shaft. On request, depressing a button on the scanner's GUI ("FC"; Fig. 5, step 1) initiated acquisition and storage of the projection images to a depository (step 2). The images were transferred and displayed on a separate PC using a custom user interface (step 3). The catheter was located on the projections either manually or automatically (step 4). A new plane was calculated and fed back to the scanner using the modified real-time interface that accepted externally defined scan planes, driving the scanner to the catheter plane (step 5). The current plane's orientation with the initially specified target plane was calculated and displayed (step 6). The catheter plane, which is displayed on the scanner (Fig. 6a), and the calculated angle allowed the physician to rotate the catheter accordingly. After subsequent confirmation that the catheter was in fact coplanar with the vessels, a standard nitinol guidewire (EV3) with a sharpened tip was coaxi-

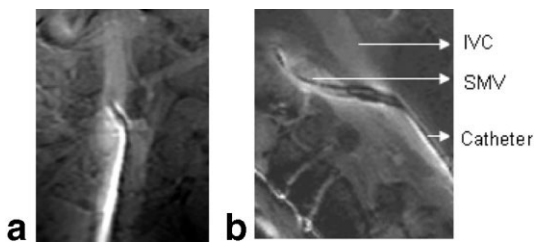

Figure 6. a: Scan plane automatically adjusted to contain the entire catheter. **b:** Puncture from the IVC to the SMV.

ally introduced through the lumen of the active needle to facilitate the puncture. The entire system (sharpened needle and active needle) was then advanced as a unit from the IVC until the SMV was entered (Fig. 6b).

Using automatic detection, we detected and drove the scanner to the catheter plane in about four seconds (approximately three seconds were spent on selecting relevant GUI buttons, and about one second was spent on the actual algorithm), which comprised the steps shown in Fig. 5. Automatic detection was implemented as an experimental feature and therefore required the selection of suitable buttons to initiate the detection. Manual detection, wherein the user identified three salient points on the catheter body, required ~10 seconds. User-initiated scan plane updates were preferred to repeated automatic updates, which can be distracting to the physician. The time required to obtain projection images depends on the imaging parameters and resolution desired. One in vivo procedure was performed completely with manual detection, and the images were used to compute automatic detection parameters as outlined above.

The plane-finding algorithm was used 15 times over the course of the two experiments. It was useful for guiding the two different catheters used in the experiments (one very rigid needle for the puncture and another, slightly flexible and curved needle for post-puncture navigation). Automatic detection, which utilized the needle dimensions, was used primarily for the puncture and successfully calculated the plane in six passes. Although finding the catheter plane was useful during the entire procedure, display of its orientation with respect to the target plane was most useful at the point of puncture and was not extensively used otherwise.

DISCUSSION

We have described and implemented a system to track the plane of an active loopless-antenna needle in a mesocaval puncture procedure performed in vivo. The scan plane was automatically adjusted and its relation to a previously acquired target plane was determined. The algorithm took advantage of the characteristic properties of the needle (i.e., it is a rigid, linear, active device with a portion of interest lying in a particular plane).

The scan plane was calculated using three points on projection images of the catheter. The points can be chosen dynamically by the user, and any relevant portion of the catheter can be tracked. The algorithm can be made more robust by considering multiple points around the catheter's tip and calculating a best-fit plane that passes through these points.

Devices used in other procedures may not share our needle's characteristics. They may not be as rigid, may involve loops, or may have no portion lying in a plane. However, algorithms may be used to compute the entire 3D shape from device projections (16,17), and a portion of interest can be viewed by adjusting the slice thickness as well as the transformation matrix. The 3D shape can also be combined, possibly not in real time, with volumetric MRI to provide a complete map of the catheter in the tissue of interest.

The target plane, as defined in this procedure (Fig. 2), shared an axis with the catheter plane along the catheter's body, and a simple rotation by the calculated angle made the needle coincident with the target plane. If there is no common axis, a single angle is insufficient and the exact relationship between the planes must be calculated and displayed. While in-plane display was useful for the current experiment, different procedures may benefit from the display of other plane orientations. Once the device plane is calculated, the scanner can easily be driven to other orientations with respect to the device by a simple change of the transformation matrix.

The earlier navigation technique used in this procedure consisted of manual determination of the catheter position in a set of multislice images. The catheter's relation to the target position was then visually determined. This cumbersome navigation, which was a crucial part of the procedure, requires considerable experience and can result in overall durations ranging from 10 to 40 minutes (1). The direct identification of catheter and target planes provided by our algorithm reduced this to ~5–10 minutes. Furthermore, our approach can simplify procedures for interventionalists who are inexperienced with complicated multiplanar imaging.

We used a simple contrast detection scheme for automatic catheter detection that performed fairly well, given prior in vivo image characteristics. However, the algorithm was sensitive to various parameters (e.g., window length), and was unreliable when large changes occurred between the prior and real-time data sets. Although it was slower, the manual approach was maintained as a robust alternative. Better algorithms, which may be computationally more intensive, should be explored for completely automatic detection.

The algorithm time (four seconds and 10 seconds for automatic and manual detection, respectively) may seem long compared to the times reported for other methods (e.g., Ref. 8). However, this increase is encountered only when explicit plane-tracking is required for navigation and not during the entire course of the experiment. Furthermore, our approach facilitates the 3D localization of every point along the catheter without making design changes to the catheter body, while the plane-computation time remains essentially the same. The total time can be reduced by integrating the algorithm into the scanner's software and by better design of the user interface.

Gradient nonlinearities can affect the correspondence between orthogonal projections. However, the in vivo and phantom experiments were performed close to the center of the magnet, where gradient nonlinearities are lowest, and we assumed that the correspondence was not substantially affected.

The interventional device used in this experiment was an active loopless-antenna catheter. However, the same algorithm can be used with other devices that cast linear projections. For example, an elongated loop coil (5) would cast projections that are almost linear when the distance between the loops is small. The method is not limited to active probes. For example, a passive metallic

probe filled with perfluorooctylbromide, when combined with fluorine NMR (19), could also be located since the projection of such a probe would appear as a bright line against a dark background.

In conclusion, we have described an image-based method to determine the orientation and image the plane of interventional devices without the need for localizing coils. The method was demonstrated in an in vivo mesocaval puncture procedure. Previously, navigation in this procedure required acquisition of multislice images of the catheter and determination of the catheter position in complex anatomy. This cumbersome navigation mandated a more efficient approach. In the present method, we directly determine the plane of the catheter using two projection images, drive the scanner to that plane, and calculate its orientation with respect to a target plane, thus aiding in the navigation of a successful procedure. We believe that this method will be useful not only for the mesocaval puncture procedure but also for many other procedures that require the catheter position to be determined quickly and accurately.

ACKNOWLEDGMENTS

We thank Dan Rettman and Mike Guttman for helpful discussions, the anonymous reviewers of this journal for their suggestions, Mary McAllister for editorial assistance, and Dr. Paul Bottomley for supporting the project.

REFERENCES

1. Arepally A, Karmarkar PV, Weiss C, Atalar E. Percutaneous MR imaging-guided transvascular access of mesenteric venous system: study in swine model. Radiology 2006;238:113–118.
2. Lederman RJ. Cardiovascular interventional magnetic resonance imaging. Circulation 2005;112:3009–3017.
3. Omary RA, Unal O, Koscielski DS, et al. Real-time MR imaging-guided passive catheter tracking with use of gadolinium-filled catheters. J Vasc Interv Radiol 2000;11:1079–1085.
4. Unal O, Li J, Chen W, et al. MR-visible coatings for endovascular device visualization. J Magn Reson Imaging 2006;23:763–769.
5. Atalar E, Bottomley PA, Ocali O, et al. High resolution intravascular MRI and MRS by using a catheter receiver coil. Magn Reson Med 1996;36:596–605.
6. Ocali O, Atalar E. Intravascular magnetic resonance using a loopless catheter antenna. Magn Reson Med 1997;37:112–118.
7. Ackerman JL, Offutt MC, Buxton RB, Brady TJ. Rapid 3D tracking of small RF coils. In: Proceedings of the 5th Annual Meeting of SMRM, Montreal, Canada, 1986 (Abstract 1131).
8. Dumoulin CL, Souza SP, Darrow RD. Real-time position monitoring of invasive devices using magnetic resonance. Magn Reson Med 1993;29:411–415.
9. Bock M, Volz S, Zühlsdorff S, et al. MR-guided intravascular procedures: real-time parameter control and automated slice positioning with active tracking coils. J Magn Reson Imaging 2004;19:580–589.
10. Elgort D, Wong E, Hillenbrand C, Wacker FK, Lewin JS, Duerk JL. Real-time catheter tracking and adaptive imaging. J Magn Reson Imaging 2003;18:621–626.
11. Qiu B, Karmarkar P, Brushett C, et al. Development of a 0.014-inch magnetic resonance imaging guidewire. Magn Reson Med 2005;53:986–990.
12. Atalar E, Kraitchman DL, Carkhuff B, et al. Catheter-tracking FOV MR fluoroscopy. Magn Reson Med 1998;40:865–872.
13. Guttman MA, Lederman RJ, Sorger JM, McVeigh ER. Real-time volume rendered MRI for interventional guidance. J Cardiovasc Magn Reson 2002;4:431–442.
14. Dick AJ, Guttman MA, Raman VK, et al. Magnetic resonance fluoroscopy allows targeted delivery of mesenchymal stem cells to infarct borders in swine. Circulation 2003;108:2899–2904.
15. Gonzales R, Wood R. Digital image processing. 2nd ed. Reading, MA: Addison Wesley; 2001. p 52.
16. Solaiyappan M, Lee J, Atalar E. Depth reconstruction from projection images for 3D visualization of intravascular MRI probes. In: Proceedings of the 7th Annual Meeting of ISMRM, Philadelphia, PA, USA, 1999 (Abstract 483).
17. Lee JS. Post processing for the real-time visualization of the intravascular MR images. M.S. thesis, Johns Hopkins University, 1999.
18. Hill FS. Computer graphics using OpenGL. 2nd ed. Upper Saddle River, NJ: Prentice Hall; 2000. p 209–286.
19. Kozerke S, Hegde S, Schaeffter T, Lamerichs R, Razavi R, Hill DL. Catheter tracking and visualization using 19F nuclear magnetic resonance. Magn Reson Med 2004;52:693–697.